

Influence of the Binder Structure on the Interfacial Adhesion and Antimigration Properties of the Propellant Charge

Bowen Zhang, Shen Yuan, Rui Ren, Zhaobo Zhang, and Yunjun Luo*

Cite This: *ACS Omega* 2022, 7, 6335–6344

Read Online

ACCESS |



Metrics & More

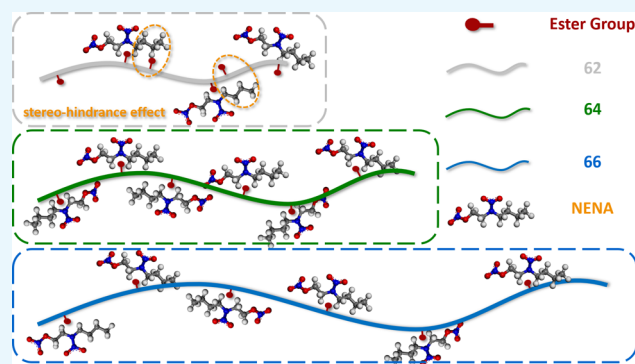


Article Recommendations



Supporting Information

ABSTRACT: Maintaining the structural integrity of solid rocket propellant charges has been widely concerned by scholars around the world. The introduction of a polyester transition layer between the propellant and the liner is a new and effective method used to improve the interfacial bonding properties of the solid propellant charge and inhibit the migration of high-energy plasticizers. Uniaxial tensile pull-off specimens and accelerated aging experiments at multiple temperatures were used to study the interfacial bonding properties of propellant charges and the migration properties of plasticizers, respectively. The influence of the polyester structure on the two properties was also discussed in detail, and a targeted antimigration mechanism was proposed based on the molecular structure of the plasticizer. In addition, the Weibull model was used to fit the plasticizer migration behavior, and the plasticizer migration master curve in the charge system was obtained based on the principle of time–temperature superposition, which broadens the application field of the model and is important from an application perspective.



1. INTRODUCTION

Solid rocket propellant is widely used in various weapons and equipment. It is the power source of tactical and strategic missiles and has an indispensable position in the defense industry. With the continuous development of weapons and equipment, countries continue to put forward higher requirements for the energy performance and safety performance of weapons and equipment. So, high-energy insensitive propellants have become a current research hotspot.¹

Compared with the traditional hydroxyl-terminated polybutadiene (HTPB) propellant, many polar substances were used in the new high-energy insensitive propellant to increase the energy performance, such as energetic binders and energetic plasticizers. However, this also leads to a large difference in polarity between the propellant binder system and the outer HTPB liner. The huge difference in polarity between the two materials will cause poor interfacial bonding performance, which can easily result in casualties, damage to weapons, and equipment during storage and application. At present, improving the interfacial bonding performance of the charge has become one of the urgent needs for the development of solid rocket motor technology.

To obtain excellent low-temperature mechanical properties, the plasticization ratio of high-energy insensitive propellants is usually much higher than HTPB propellants, which will lead to a greater tendency of energetic plasticizers to migrate to the outer coating material. Unlike the migration of traditional inert plasticizers (such as small molecule esters, dioctyl phthalate,

dioctyl sebacate, etc.), the migration of energetic plasticizers (such as *N*-butyl-*N*-nitroethyl nitramine) will cause deviation of the energy performance of the propellant from the theoretical value, affecting the internal ballistic performance,² and influence the stability of the propellant combustion.³ In addition, since such energetic plasticizers usually contain nitrate ester groups which are unstable and have an autocatalytic decomposition effect, they will accelerate the decomposition and fracture of the main chain structure in the migration area.⁴ Finally, the enrichment of the plasticizer at the interface will destroy the nonbonding force between the two phases and form a softened layer.^{5,6} It is a key issue that the migration of energetic plasticizers in propellants should be reduced.

At present, scholars are trying methods to improve the bonding performance of the charge interface, such as increasing the concentration of interface reactive groups,⁷ introducing bonding agents into the liner,⁸ and increasing the interface roughness.^{9,10} Although these methods can indeed improve the initial bond strength of the system, the long-term

Received: December 7, 2021

Accepted: February 2, 2022

Published: February 14, 2022



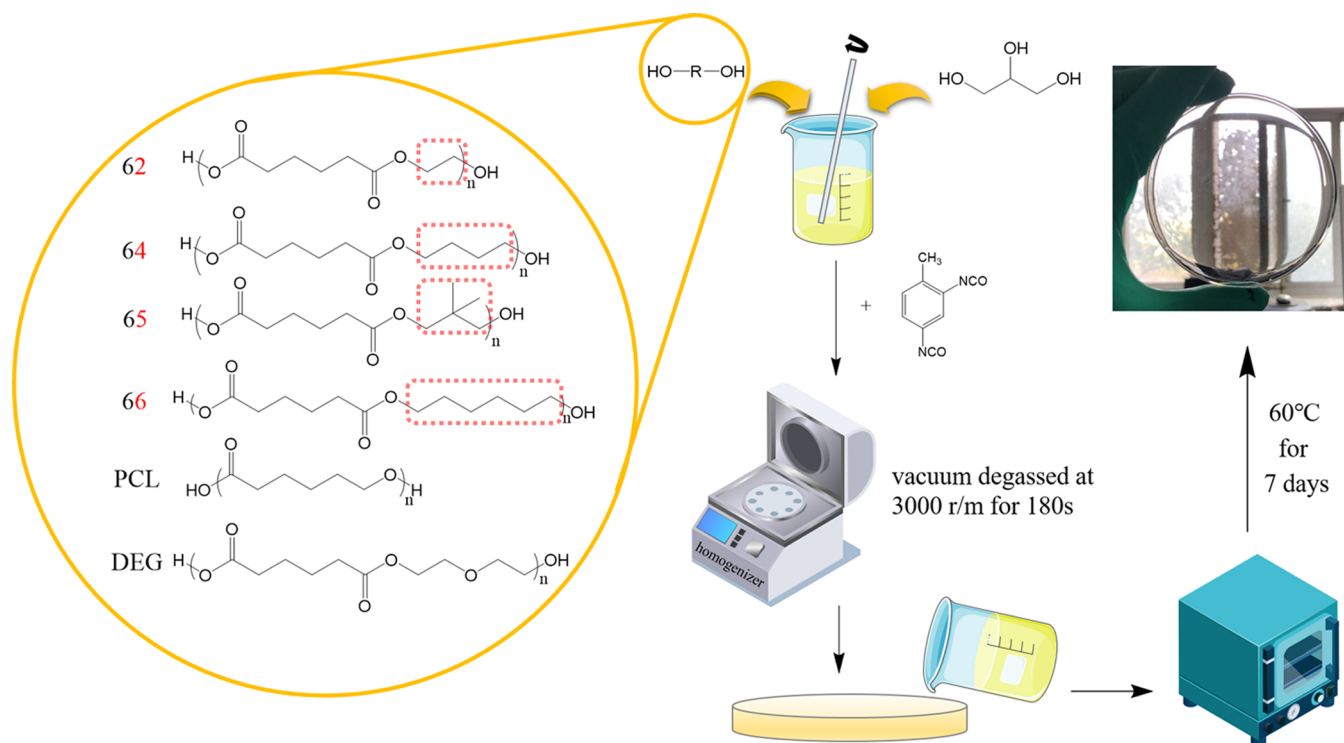


Figure 1. The preparation process of the transition layer.

migration of plasticizers will have a serious negative impact on the bonding performance as the aging time increases.¹¹ The research on improving the antimigration performance is mainly focused on the modification of migrant molecules,^{12–14} increasing the cross-linking density of coating materials,^{3,15–17} adding antimigration fillers,¹⁸ etc. However, there are few studies on the influence of the binder backbone structure on migration resistance.

As a commonly used adhesive material, polyurethane has been widely used in aerospace, weapon science, and other fields. The characteristics of soft and hard segments can lead to excellent bonding properties and mechanical properties in a wide temperature range. Since PU is used in composite solid propellant as the binder matrix, materials with the same curing system can have the best compatibility and interface properties.¹⁹ To obtain the binders with the best overall performance, this paper first studies the interfacial adhesion properties and antimigration properties of the transition layers made of six commonly used hydroxyl-terminated polyesters. Second, the Weibull model is used to fit the migration behavior of plasticizers. Finally, the NENA migration master curve in the corresponding material is obtained.

2. MATERIALS AND METHODS

2.1. Materials and Preparation of the Transition Layer. In this paper, six hydroxyl-terminated polyesters were used to prepare their respective transition layers: polyethylene adipate (62), polybutylene adipate (64), polyhexylene adipate (66), polyneopentyl adipate (65), polycaprolactone (PCL), and poly(diethylene glycol adipate) (DEG). The above materials are all provided by Xuchuan Chemical Co., Ltd, and their molecular weight is 2000 g/mol. The adhesives should be dewatered in a vacuum drying oven at 60 °C for more than 12 h.

The molar ratio of -NCO/-OH of the reactants in all transition layer formulations was 1.5 (in the polyurethane industry, the ratio is usually named *R* value, that is, *R* = 1.5) and the molar ratio of toluene diisocyanate/glycerin = 3, which is the optimized result of our previous work.²⁰ When preparing the transition layer film, first, stoichiometric amounts of the polyester binder and glycerin (AR, Sarn Chemical Technology Co., Ltd.) were added to the beaker, and stirred well at 60 °C. Then, a stoichiometric amount of toluene diisocyanate (TDI, Tianjin Guangfu Fine Chemical Research Institute) and 0.3 wt % catalyst (dibutyltin dilaurate/triphenylbismuth = 1:2, both diluted with dioctyl sebacate (DOS) to a solution with a concentration of 0.5% in advance; dibutyltin dilaurate and triphenylbismuth were obtained from Beijing Chemical Plant and DOS was from Luoyang Liming Chemical Research Institute) were added, stirred manually with a glass rod for 3 min, and then placed in a homogenizer, and vacuum degassed at 3000 r/m for 180 s. After the defoaming was completed, the transparent and clear transition layer slurry was poured into a polytetrafluoroethylene mold and placed in a 60 °C thermostat to cure for 7 days. After curing was completed, it could be demolded to obtain a polyester transition layer. The entire preparation process is represented in Figure 1.

The components of the HTPE propellant and HTPB liner involved in the experiment were all provided by Xi'an North Hui'an Chemical Industry Co., Ltd. The amount of NENA added to the propellant is 11 wt %. The specific formulation of the propellant is inconvenient to disclose due to sensitive reasons.

2.2. Mechanical Analysis. 2.2.1. Preparation of Adhesive Specimens and Adhesive Test Conditions. First, the standard metal bases with the HTPB liner slurry, about 1.5–2.0 mm thick, were coated. When it was naturally leveled, the bases were placed into a 70 °C thermostat for a 24 h pre-curing process. After the pre-curing was completed, the liner had a

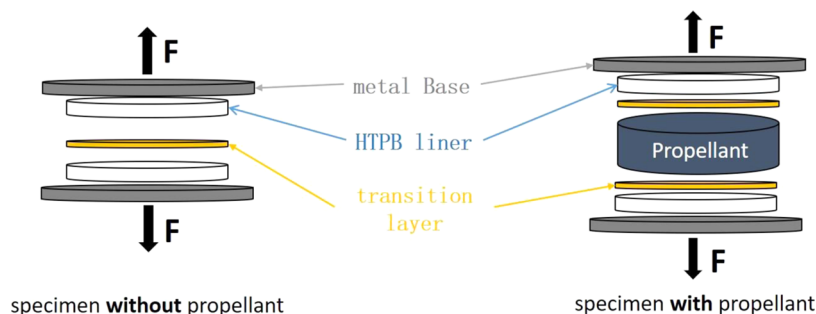


Figure 2. Schematic diagram of two adhesive specimens.

certain resistance to deformation, but the surface was still sticky. Subsequently, the pre-mixed transition layer slurry was uniformly scraped on the liner with a thickness of about 0.5 mm and placed into a 60 °C thermostat for pre-curing for 24 h. After the pre-curing was completed, the metal bases with the liner/transition layer were assembled with other molds and placed in a vacuum environment. The propellant slurry was cast from the casting port, and finally, those adhesive specimens were placed in a 60 °C thermostat for the co-curing process. After curing for 7 days, the adhesion test samples could be obtained (Figure 2, right). Another type of adhesive specimens without the propellant were prepared by omitting the step of casting propellant, which can be obtained by co-curing the liner and the transition layer directly in the corresponding mold (Figure 2 left).

The test used an electronic universal tensile testing machine (Shimadzu, WD-4005) with a joint tensile rate of 20 mm/min, 25 °C. Bond strength was determined as the maximum tensile strength.

2.3. Contact Angle Test. The sample was placed on the sample table of the JY-82 contact angle tester, and the contact angles of three reference liquids (diiodomethane, formamide, water) on the surface at 20 °C were tested. Each group of samples is tested five times in parallel, and the average value of the contact angle is taken, and the error is within 2°. Formula 1–3 are used to calculate the surface energy of the material and the work of adhesion (W_a) with the propellant fillers.²¹

$$\gamma_1(1 + \cos \theta) = 2(\gamma_s^d \gamma_1^d)^{1/2} + 2(\gamma_s^p \gamma_1^p)^{1/2} \quad (1)$$

$$\gamma_{sl} = [(\gamma_1^d)^{1/2} - (\gamma_s^d)^{1/2}]^2 + [(\gamma_1^p)^{1/2} - (\gamma_s^p)^{1/2}]^2 \quad (2)$$

$$W_a = \gamma_s + \gamma_1 - \gamma_{sl} \quad (3)$$

where γ_{sl} is the interfacial tension between the two phases, γ_s^d and γ_1^d are the surface tension of the two phases separately, γ_s^p and γ_1^p are the dispersion surface tensions of the two phases separately, and γ_s^p and γ_1^p are the dipolar surface tensions of the two phases separately.

2.4. Plasticizer Analysis. **2.4.1. Sample Preparation for the Sandwich Method.** The samples of the sandwich method adopted the sandwich structure of liner/transition layer/propellant/transition layer/liner and were completely wrapped with aluminum foil to reduce the effect of NENA volatilization. A weight of 500 g was placed over each set of samples to ensure close contact between the layers. The propellant used a $\phi 30$ mm propellant grain with a thickness of about 10 mm, the transition layer used a $\phi 30$ mm sheet with a thickness of about 1 mm, and the liner used a $\phi 30$ mm HTPB sheet with a thickness of about 1.5 mm. Samples were placed at 40, 50, 60,

and 70 °C for migration experiments. In addition, the samples without polyester transition layers were also prepared at the corresponding temperature to study the effect of introducing transition layers on the migration of NENA.

2.4.2. Concentration of NENA in the Sample Obtained by Extraction-Chromatography. Propellant, liner, and transition layer test samples were manually cut into pieces of 2 mm \times 2 mm \times 1 mm. The small piece was immersed in 25 mL of methanol (chromatographically pure, Sigma Aldrich) separately for a 24 h room temperature extraction. Then, the extract was transferred to a 50 mL volumetric flask and made up to volume. The prepared solution samples were injected into a HPLC system (LC-20AD, Shimadzu, Japan) that had been previously calibrated by an external standard method through a 25 μ L injection needle, and the test conditions were as follows: the flow ratio of methanol/water = 8:2, a total flow rate of 1 mL/min, UV detector SPD-20 wavelength of 254 nm, and shim-pack VP-ODS (5 μ m, 4.6 mm \times 250 mm). Under these conditions, the NENA peak appeared at around 4.62 minutes. The concentration of NENA in the sample can be calculated from

$$c_x = \frac{c_{xd} * V_x}{m_x} \quad (4)$$

where c_x is the concentration of NENA in the corresponding sample, mg/g; c_{xd} is the NENA concentration determined by HPLC, mg/mL; V_x is the total volume of the sample solution, mL; m_x is the mass of the sample, g.

2.4.3. Mathematical Treatment. To better describe the migration behavior of NENA in different materials, it is necessary to fit the relevant migration data with a suitable model. At present, scholars mainly adopt two types of migration models: one is the traditional migration model based on Fick's law. This model has more prerequisites and the simulated situation is more ideal. This model has been widely used in the field of solid propellant plasticizer migration^{3,22,23} and can be described by eq 5²⁴

$$\frac{M_t}{M_\infty} = 1 - \frac{8}{\pi^2} e^{(-\pi^2 D t / L^2)} \quad (5)$$

where L is the thickness (mm) of the migrated material, t is the migration time (s), and D is the diffusion coefficient (mm²/s). M_t is the mass (mg) of NENA transferred into the coating material at time t ; M_∞ is the mass (mg) of NENA transferred into the coating material at equilibrium.

The concentration of NENA (%) in the coating material is defined using $c_t = \frac{M_t}{M_p}$, $c_\infty = \frac{M_\infty}{M_p}$, unit is mg/mg, where M_p is

the mass of the coating material (mg), then the formula (5) can be written as

$$\frac{c_t}{c_\infty} = 1 - \frac{8}{\pi^2} e^{(-\pi^2 D t / L^2)} \quad (6)$$

The other is the Weibull model, which was first proposed by Weibull in 1939.²⁵ It is a probability density function used to study the failure time distribution and it can also be used to study the diffusion of pollutants in the atmosphere and many other issues.²⁶ The Weibull model has relatively few restrictions and can simulate more complex migration behaviors that are closer to the actual situation. In recent years, the Weibull model is often used to describe the migration behavior of small molecules in food packaging materials^{27–31} and there is no report on the application of this model in the migration of propellant plasticizers.

Since the initial content of NENA in the coating materials involved in this article is 0 mg/L, the Weibull model can be written as

$$c(t) = c_\infty - c_\infty * e^{-(t/\tau)^\beta} \quad (7)$$

where c_t is the NENA content in the outer coating material (transition layer, liner) at time t ; c_∞ is the NENA content in the outer coating material when the migration equilibrium is reached, τ is the system time constant and is related to the diffusion rate, and the shape parameter β is a function of the interface mass transfer resistance, and its value is related to the temperature, the molecular structure of migration, physical and chemical properties, and the initial concentration.

3. RESULTS AND DISCUSSION

3.1. Propellant/Transition Layer Interface Bonding Properties. The introduction of the transition layer between the propellant and the HTPB liner is mainly to improve the interfacial bond strength of the system, so the surface properties of different materials need to be characterized first. The surface tension of each coating material, as well as the interfacial tension and adhesion work with AP and RDX are respectively listed in Table 1. P is used to characterize the

Table 1. Interfacial Tension and Adhesion Work between the Binder System and AP and RDX

	P	γ_L (mN/m)	γ_{SL} (mN/m) (RDX)	W_a (mN/m) (RDX)	γ_{SL} (mN/m) (AP)	W_a (mN/m) (AP)
HTPB liner		37.52	9.57	85.67	22.65	57.77
DEG	4.33	53.88	6.52	105.09	23.69	73.09
62	5	53.25	10.86	100.12	30.22	65.92
64	6	50.64	5.35	103.02	20.73	72.81
65	5.5	53.10	8.72	102.10	26.99	69.01
66	7	44.59	10.33	92.00	26.62	60.87
PCL	7	46.07	6.35	97.45	20.92	68.05

content of polar groups, its value = (the number of atoms in the main chain of the repeating unit)/(the number of polar groups in the repeating unit). The smaller the value of P , the denser the polar sites. The detailed structure of each polyester binder has been shown in Figure 1.

It can be seen from the data in the table that due to the low polarity of HTPB, its surface tension and adhesion work are significantly lower than those of various polyester materials.

Among the six polyester materials, the surface tension of the material is greatly affected by the content of polar groups (P). The higher the content of polar groups, the greater the surface tension, which is more conducive to the formation of nonbonding interactions at the interface. DEG has the highest content of polar groups among the six polyesters, so it has the highest surface tension and adhesion to oxidant fillers.

Second, bonding performance of the bonded specimens without propellant (Figure 2 left) is tested to ensure that the other interfaces in the system are well bonded. The test results are shown in Table 2. It can be seen from the table that as the

Table 2. Influence of the Binder of the Transition Layer on the Bond Strength

(shell–liner–transition layer)	
transition layer composition	bond strength (MPa)
DEG ($R = 1.5$)	1.40
62 ($R = 1.5$)	2.03
64 ($R = 1.5$)	1.80
65 ($R = 1.5$)	1.79
66 ($R = 1.5$)	1.66
PCL ($R = 1.5$)	1.62

content of polar groups in the adhesive decreases, the nonbonding force between the two phases gradually weakens, resulting in the decrease of the bonding performance. In addition, a certain degree of crystallinity of the binder is beneficial for the bonding performance,³² and all polyesters except DEG have certain crystalline properties. Therefore, the bond strength of the bonding test piece using the DEG transition layer is the lowest. The bond strength of all systems is significantly higher than the strength of the HTPB composite solid propellant (about 0.9–1.0 MPa), so it will not cause debonding due to poor mechanical properties of the bonding material itself or low bond strength of other interfaces in the system.

Table 3 shows the influence of the transition layer on the interface bond strength of propellant-bound specimens. It can

Table 3. Influence of the Binder of the Transition Layer on the Bond Strength^a

(shell–liner–transition layer - propellant)	
transition layer composition	bond strength (MPa)
without transition layer	0.14
DEG transition layer	0.64
62-transition layer	0.62
64-transition layer	0.60
65-transition layer	0.58
66-transition layer	0.47
PCL transition layer	0.46

^aThe strength of the propellant is 0.9 MPa.

be seen from the table that when the polyester transition layer is not used in the bonding specimen, the bond strength is only 0.14 MPa, indicating that the bonding performance is very poor, and the failure interface is smooth and flat with a large area of the exposed HTPB liner (Figure 3a). After introducing the polyester transition layer between the propellant and the liner, the bond strength of the system is greatly improved, up to 0.64 MPa, and the broken section is rough and attached with the propellant (Figure 3b), indicating that the bonding

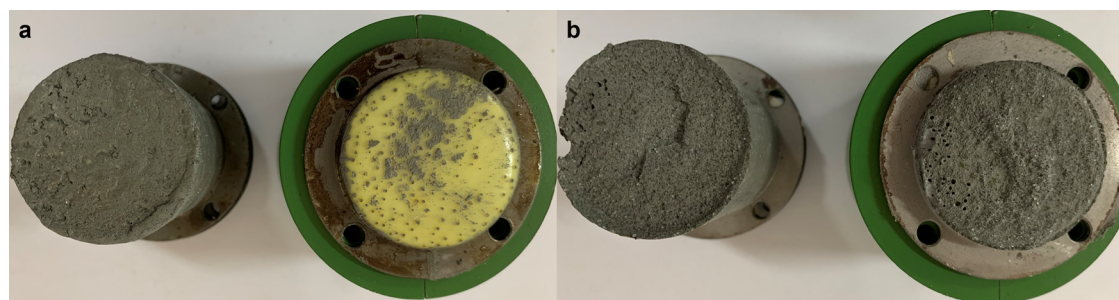


Figure 3. Fracture surfaces of bonding test specimens before (a) and after (b) the introduction of the transition layers.

performance is good. As the content of polar groups in the polyester decreases, there is also a tendency of the bond strength to gradually decrease, indicating that increasing the number of polar groups is beneficial to improving the interfacial bonding performance.

It is worth noting that the DEG transition layer has the strongest bond strength among the bonded specimens containing the propellant, while the results are completely opposite in the bonded specimens without the propellant. This is mainly because the curing process of the propellant-bound specimens is very complicated, and the bond strength is not only related to the transition layer formulation but also affected by the migration of plasticizer molecules in the propellant.

Although the fracture occurred at the interface propellant after the introduction of the transition layer, the interface bond strength was still lower than the bulk strength of the propellant. This shows that the main reason for the fracture is that the enrichment of NENA in the interface area leads to a decrease in the strength of the interface propellant.

We cut the propellant part of the bound specimen and found that the energetic plasticizer NENA in the propellant is enriched at the propellant/transition layer interfaces (Figure 4), which can decrease the strength of the interfacial



Figure 4. NENA enrichment in the interfacial propellant area.

propellant, and even affect its complete curing, resulting in a softened layer.³³ In addition, the enrichment of the plasticizer at the interface will also lead to the destruction of the no-bonding force between the two layers, thus inhibiting the migration of NENA is also important for improving the bonding performance.

3.2. Effect of the Transition Layer on Migration Behavior of the Plasticizer. The commonly used “sandwich method” is used to study the influence of the binder matrix on the antimigration properties of the material. Accelerated aging experiments were carried out at 40, 50, 60, and 70 °C, and the NENA content in the material was quantitatively monitored through extraction-chromatography on a regular basis. The results of the migration experiment are shown in Figure 5. The solid line in the figure is the theoretical value obtained through

the Weibull model, and the relevant parameters obtained by fitting are summarized in Tables S1–S4.

It can be seen from Figure 5 that the tendency of NENA to migrate into the transition layer at each temperature shows the following trend: as the migration time increases, the migration rate gradually slows down, and finally reaches a migration equilibrium. The higher the temperature, the shorter the time required for migration to reach equilibrium. The migration equilibrium concentration of the same sample at different temperatures is almost the same, which indicates that temperature affects only the kinetic process of migration and has little effect on the thermodynamic process.

During the migration process, we observed the phenomenon that the plasticizer caused the swelling of the surface of the transition layer (Figure 6), which indicates that the entire migration process is not only controlled by the diffusion process, and does not meet the prerequisites for applying Fick's law,³⁴ causing the fitting result of Fick's law to deviate from the experimental value. However, due to various reasons such as the properties of the material and the test temperature, the fitting deviation is not very large, and Fick's model can still be used. Therefore, most of the current research related to migration and diffusion is still using Fick's model.

The assumption that the migrated material does not swell during the migration process is too ideal, which leads to obvious limitations in Fick's model in some cases, such as the epoxy transition layer currently being studied by our research group. Since the glass transition temperature of the studied epoxy resin material is higher than the migration experiment temperature and the material itself is a rigid material with a high cross-linking density, the migration process of the plasticizer is relatively more complicated. As shown in Figure 7, the entire migration process experiences three processes: initial slow migration, swelling-accelerated migration, and finally reaching a migration equilibrium. If the above migration trend is fitted with Fick's model, a huge deviation will occur (Figure 7a) because the model defaults that the material will not swell during the entire migration process. In fact, the glass transition temperature of epoxy materials gradually decreases with the continuous migration of plasticizers, until it drops below the test temperature and presents a highly elastic state. The significant improvement in the chain motion ability is an important reason why the overall migration trend shows an S-shape. Eventually, due to the decrease in the concentration gradient, the migration gradually stabilizes until the migration equilibrium is reached. Compared with the fitting results, the Weibull model used in the whole migration process has a much better degree of fit.

The β parameter in the Weibull model can well describe the migration phenomenon with relaxation. The smaller the β

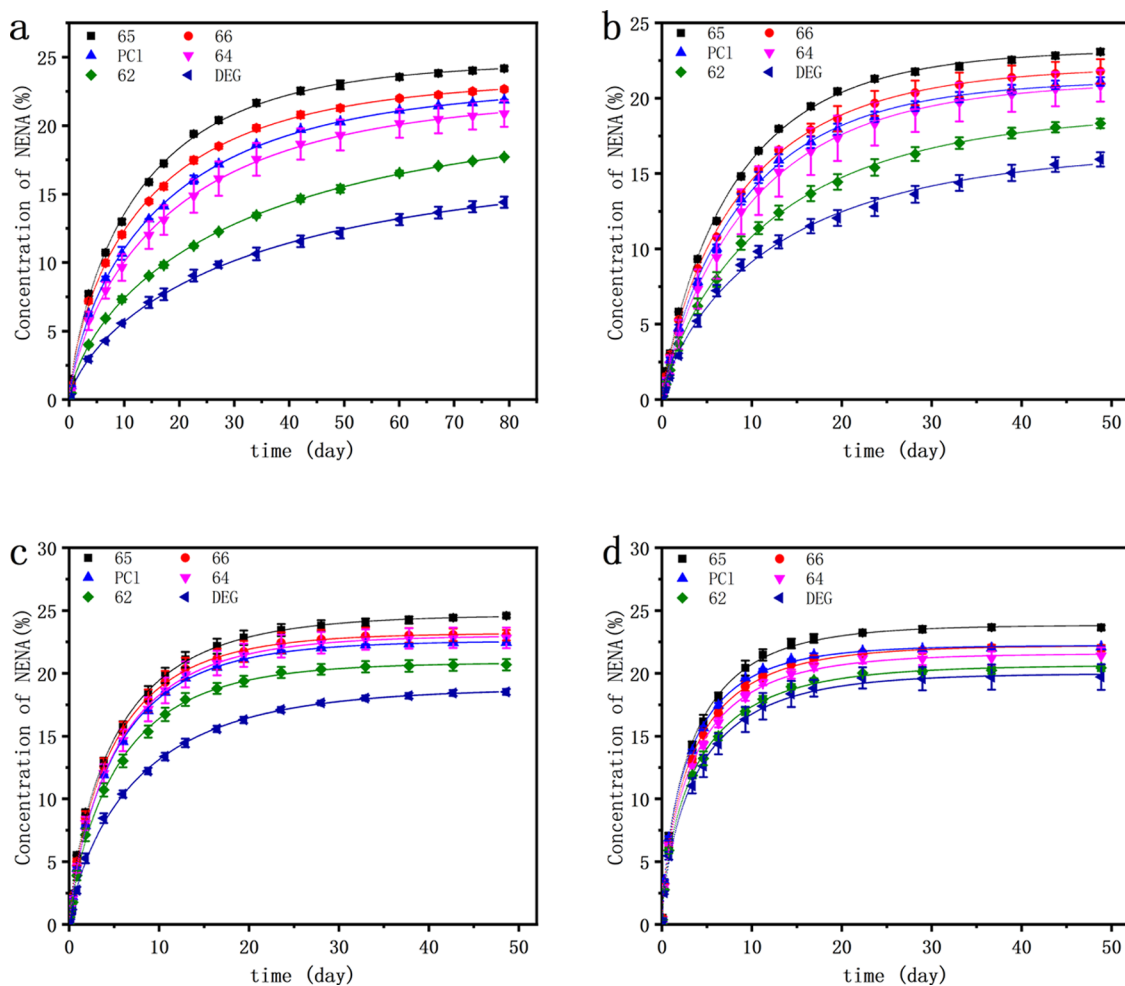
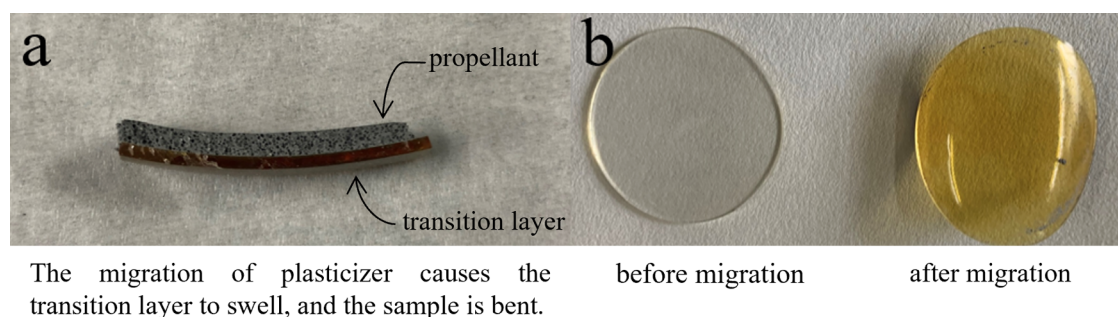


Figure 5. Trend of NENA migration in the polyester transition layer over time (experimental temperature, (a) 40 °C; (b) 50 °C; (c) 60 °C; (d) 70 °C).



The migration of plasticizer causes the transition layer to swell, and the sample is bent.

before migration after migration

Figure 6. Migration of plasticizer causes the transition layer to swell ((a) partially sandwiched migration samples; (b) difference in appearance before and after NENA moves into the transition layer).

value, the more obvious the relaxation phenomenon. From the fitting results of the two models, the Weibull model has a better fit (R^2 stands for the fitting correlation coefficient), so we believe that this model can better describe the migration behavior of the plasticizer in the propellant charge system (especially for those systems with higher plasticization). At present, there is no report that the Weibull model has been used to study the migration behavior of plasticizers in propellants. This is a meaningful expansion of the application field of the Weibull model.

The amount of migration can also be affected by the cross-linked network structure of the material. We tested the

migration of NENA in the DEG transition layer with different pre-curing degrees, and the results are shown in Table 4 below. It can be seen from the table that as the pre-curing time of the transition layer increases, the amount of NENA migration gradually decreases. This is mainly because as the curing time increases, the degree of curing reaction in the transition layer becomes higher and the cross-linking density gradually increases, resulting in stronger migration resistance. In addition, the increase in the degree of curing of the transition layer will result in a decrease in the wettability of NENA on its surface, which also helps in inhibiting its further migration. However, too long pre-curing time will cause the surface of the

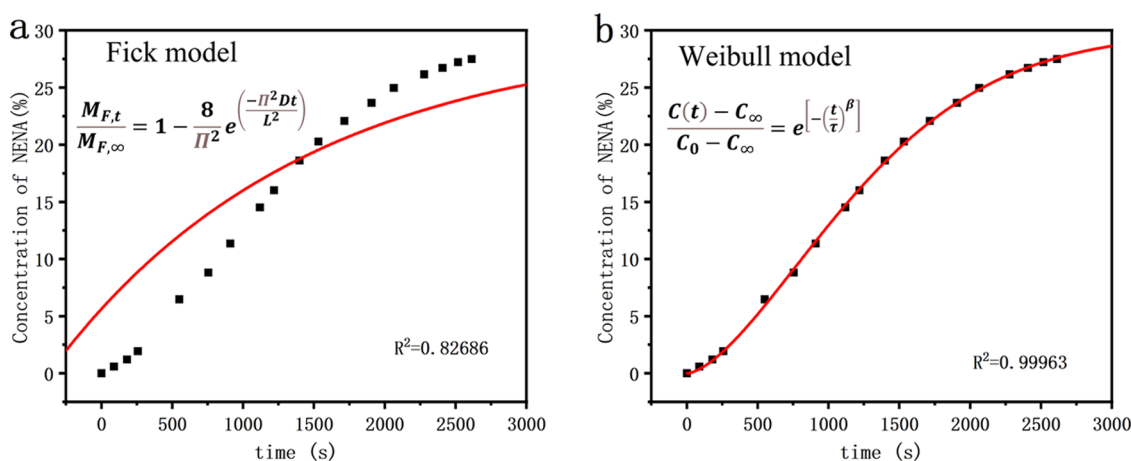


Figure 7. Fitting results of NENA migration behavior in the epoxy transition layer ((a) Fick's model; (b) Weibull model).

Table 4. Effect of the Pre-curing Time of the Transition Layer on the Migration of NENA^a

pre-curing time (60 °C)	concentration of NENA (%)	bond strength (MPa)
1 d	19.38 (±0.33)	0.64
1.5 d	17.69 (±0.03)	0.46
2 d	14.68 (±1.25)	0.21
2.5 d	13.65 (±0.15)	
3 d	13.57 (±0.14)	
5 d	11.84 (±0.15)	
7 d	11.56 (±0.50)	

^aConcentration of NENA was obtained at 60 °C for 7 days.

material to lose its viscosity, and the number of active groups is too low to form an effective covalent bond with the propellant slurry, which does not have any application prospect (samples with a pre-curing time longer than 2 days have poor interfacial adhesion and cannot be tested.). Therefore, when determining the pre-curing process, it is necessary to consider the impact on the two properties.

The regulation of NENA migration into different transition layers at different experimental temperatures is almost the same (65 > 66 ≈ PCL > 64 > 62 > DEG). Since the formulations of the transition layers are completely the same except for the different types of polyester binders, so it can be

considered that the difference in the migration degree is mainly caused by different polyester structures. The only binder with side groups among all polyesters is 65, resulting in a looser molecular chain arrangement and a larger chain-to-chain spacing, which leads to the highest amount of NENA migration in the 65-transition layer. In the immersion method, this effect is much more obvious (Figure S1), while in the sandwich method, this phenomenon is not obvious mainly because of the relatively low amount of NENA added and the limited mobility of NENA molecules.

We have confirmed that the interaction between NENA and the polar sites of the polyester matrix is a stronger migration driving force than the concentration gradient.²⁰ Therefore, for the NENA migration results of the 62, 64, and 66 “homologous” polyester transition layers, our expectation is that as the content of polar groups increases, the amount of NENA migrating into the corresponding layers will gradually increase. However, the experimental result is completely in contrast to expectations. To better explain this phenomenon, we provide an explanation from the perspective of steric hindrance. The schematic diagram is shown in Figure 8. The nitrogen atom in the nitroamine group on NENA is electropositive by the electron-withdrawing action of the nitro group, and it has strong electrostatic force with the oxygen atom of the ester group on the polyester main chain.

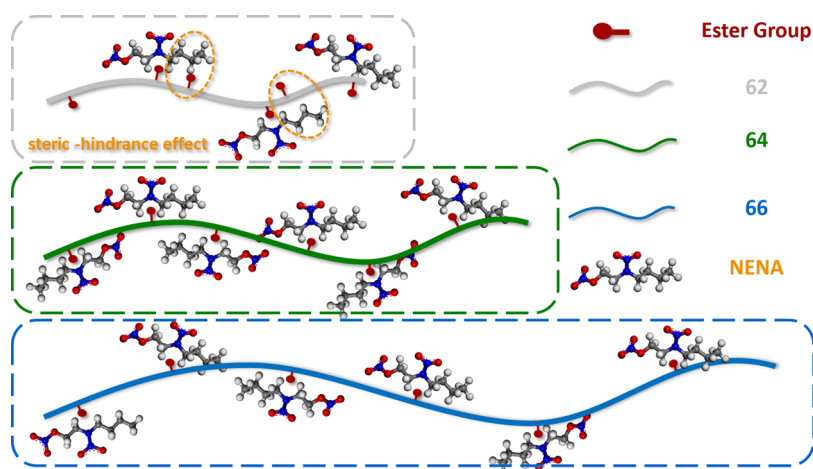


Figure 8. The steric shielding effect of NENA's butyl group on adjacent ester groups.

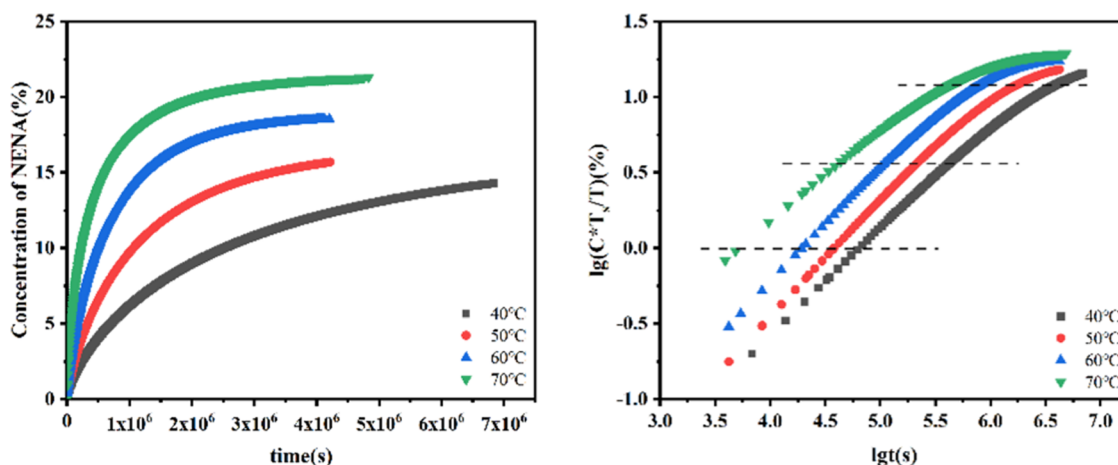


Figure 9. Change in the trend of NENA content in the transition layer with time (left); temperature–time transformation relationship (right).

However, because NENA molecule has a large butyl long chain, its existence will have a shielding effect on adjacent ester groups, especially 62 with denser ester groups. Although 62 has the largest number of polar sites, a considerable part of the sites cannot absorb NENA due to the “shielding effect”, which ultimately leads to hindered migration of NENA in the 62-transition layer. Compared with 62, the 64-ester group spacing has increased and the shielding effect is weakened, resulting in significantly higher migration of NENA in the 64-transition layer than in the 62-transition layer. If the distance between ester groups is further increased, such as 66, due to the marginal diminishing effect of the shielding effect, this factor is no longer the main factor affecting the interaction between polyester and NENA, so the amount of NENA migration in the 66-transition layer is just slightly higher than 64-transition layers.

According to the abovementioned “steric-hindrance effect”, in the system with NENA as the main migration, we can improve the antimigration performance by increasing the density of polar interaction sites; at the same time, more polar sites can increase the surface energy of the material and form more intermolecular forces with the contact material, which is also beneficial for improving the bonding force.

In fact, most plasticizers have alkyl chains, which are formed by the plasticizing mechanism of plasticizers. We can screen and modify the “plasticizer contact” materials according to the spatial structure of various plasticizers to achieve better antimigration or plasticizing effects.

3.3. Establishment of the Master Curve of Plasticizer Migration. The migration master curve can be used to predict the migration behavior of plasticizers at different temperatures and different migration times, especially for extremely long storage experiments that are difficult to be measured by experiments. Compared with the long-term storage experiment, it is more convenient and efficient to estimate the plasticizer migration behavior using the time–temperature superposition principle (TTSP), and it dramatically saves manpower, material, and financial resources, which is very meaningful.^{35,36} At present, the work carried out in related fields is mainly focused on the establishment of the master curve of various mechanical properties of propellants,^{37–39} and a few research studies on the migration properties of plasticizers are involved. However, the phenomenon of plasticizer migration is very common, and will have a non-

negligible impact on the entire charge system, so the establishment of a plasticizer migration master curve is of great significance.

From the previous research, we know that the polyester transition layer with DEG as the binder has the best bonding performance and antimigration performance, so in this section, we will establish the NENA migration master curve in the DEG transition layer. It can be clearly seen from Figure 9 that as the migration temperature increases, the migration rate increases significantly, and the time required to reach the migration equilibrium is gradually shortened. Different combinations of temperature and migration time can reach the same migration concentration, that is, the two factors time and temperature have equivalent effects on the migration of NENA, which conforms to the time–temperature superposition principle.

Generally, the experimental temperature closest to room temperature is used as the reference temperature T_s . So, 40 °C is selected as the reference temperature in this sample. The logarithm of the migration concentration was taken and plotted with the lgt to obtain four curves with parallel intervals (Figure 9 right panel). Each curve shifts to the reference temperature by lga_T to allow the two curves to overlap each other, and the distance is the displacement factor (lga_T) at each temperature. When the experimental temperature is higher than the reference temperature, the displacement factor is negative.

Plotting the displacement factors against the temperature, as shown in Figure 10, it is found that there is an obvious linear relationship.⁴⁰ The fitting coefficient is 0.993, and the fitting result is: $lga_T = -0.03375 * T + 10.59588$.

After shifting the concentration logarithm curve at each temperature to the reference temperature curve by the corresponding lga_T , the scatter plot of the master curve can be obtained, as shown in Figure 11.

From the scatter diagram, the main curve is in the logarithmic form and the following expression can effectively describe the trend. Where C is the content of NENA, T_s is the reference temperature, T is the experiment temperature, t is the migration time, and A_1 , A_2 , A_3 , and A_4 are fitting constants.

$$\log(C^*T_s/T) = A_1 + \frac{A_2}{1 + e^{(A_3 * \log(t/aT) + A_4)}} \quad (8)$$

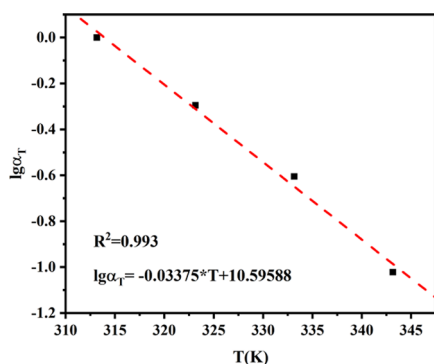


Figure 10. Relationship between the displacement factor and the experimental temperature.

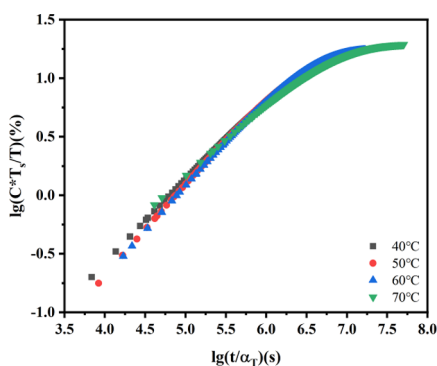


Figure 11. Scatter plot of the NENA migration master curve in the DEG transition layer.

The fitting result is shown in Figure 12, the correlation coefficient is 0.996, indicating a good degree of fitting.

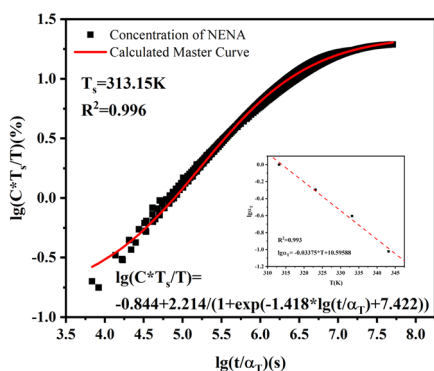


Figure 12. Fitting of the scatter plot of NENA migration master curve in the DEG transition layer.

When using the master curve to solve practical problems, first, the displacement factor $lg a_T$ corresponding to the experimental temperature T is determined from the displacement factor–temperature diagram. Then, the displacement factor $lg a_T$, the experimental temperature T , and the experimental time t are substituted into the master curve equation, and the estimated NENA migration under the corresponding experimental conditions can be obtained.

4. CONCLUSIONS

In this paper, to improve the interfacial adhesion and migration resistance, a polyester transition layer is coated between the

high-energy insensitive propellant and the HTPB liner. The interfacial bonding performance can be greatly enhanced from the initial 0.14 to 0.64 MPa by the optimization of the polyester binder. Polar interactions between the polar sites in the polyester transition layer and NENA molecules can inhibit the further migration of NENA to the outer coating material, which is the antimigration mechanism. The difference in the antimigration properties of the six types of polyester transition layers is mainly caused by the content of the main chain polar groups and the special steric hindrance of NENA, which provide theoretical support for the optimization of the binder matrix of the transition layer and any other plasticizer contact materials. The Weibull model is used to fit the NENA migration behavior, and a better fitting result than the traditional Fick model is obtained. This is the first application of the Weibull model in the field of propellant charges. Finally, according to the principle of time–temperature superposition, the master curve of NENA migration in the DEG transition layer is acquired, which can be used to estimate the plasticizer migration in a wide temperature and long-term range reasonably and has important guiding significance for practical applications.

■ ASSOCIATED CONTENT

Supporting Information

The Supporting Information is available free of charge at <https://pubs.acs.org/doi/10.1021/acsomega.1c06929>.

Migration trend of plasticizers in the immersion method and the Weibull model fitting results of the migration trend in the sandwich method (PDF)

■ AUTHOR INFORMATION

Corresponding Author

Yunjun Luo – School of Materials Science and Engineering, Beijing Institute of Technology, Beijing 100081, China; orcid.org/0000-0001-6927-2635; Email: yjluo@bit.edu.cn

Authors

Bowen Zhang – School of Materials Science and Engineering, Beijing Institute of Technology, Beijing 100081, China
Shen Yuan – School of Materials Science and Engineering, Beijing Institute of Technology, Beijing 100081, China
Rui Ren – School of Materials Science and Engineering, Beijing Institute of Technology, Beijing 100081, China
Zhaobo Zhang – School of Materials Science and Engineering, Beijing Institute of Technology, Beijing 100081, China

Complete contact information is available at:

<https://pubs.acs.org/10.1021/acsomega.1c06929>

Author Contributions

B.Z.: Methodology, formal analysis, investigation, data curation, writing manuscript, visualization. S.Y.: Supervision. R.R.: Provision of study materials. Z.Z.: Provision of study materials, investigation. Y.L.: Conceptualization, supervision.

Notes

The authors declare no competing financial interest.

All data generated or analyzed during this study are included in this published article (and its Supporting Information Files).

ACKNOWLEDGMENTS

This research did not receive any specific grant from funding agencies in the public, commercial, or not-for-profit sectors.

REFERENCES

- (1) Fu-ming, X. The Insensitive High Energy Propellants in the 21st Century [J]. *Chin. J. Explos. Propellants* **2003**, *26*, 1–4.
- (2) Pröbster, M.; Schmucker, R. Ballistic anomalies in solid rocket motors due to migration effects. *Acta Astronaut.* **1986**, *13*, 599–605.
- (3) Agrawal, J.; Agawane, N.; Diwakar, R.; Chandra, R. Nitroglycerine (NG) migration to various unsaturated polyesters and chloropolyesters used for inhibition of rocket propellants. *Propellants, Explos., Pyrotech.* **1999**, *24*, 371–378.
- (4) Huang, Z.-p.; Nie, H.-y.; Zhang, Y.-y.; Tan, L.-m.; Yin, H.-l.; Ma, X.-g. Migration kinetics and mechanisms of plasticizers, stabilizers at interfaces of NEPE propellant/HTPB liner/EDPM insulation. *J. Hazard. Mater.* **2012**, *229–230*, 251–257.
- (5) Venkatesan, D.; Srinivasan, M.; Reddy, K. A.; Pendse, V. The migration of plasticizer in solid propellant grains. *Polym. Int.* **1993**, *32*, 395–399.
- (6) Rezaei-Vahidian, H.; Farajpour, T.; Abdollahi, M. Using an inhibitor to prevent plasticizer migration from polyurethane matrix to EPDM based substrate. *Chin. J. Polym. Sci.* **2019**, *37*, 681–686.
- (7) de Moraes, A. M. F.; Pinto, J. A. R.; Holanda, J. A. S.; Gomes, P. M. d. A. E.; das Acácias, V. In *Optimization of Bondline's Properties of Solid Rocket Motors*, International Annual Conference-fraunhofer Institut für Chemische Technologie, Fraunhofer-Institut für Chemische Technologie: Berghausen, 2006.
- (8) Gercel, B.; Üner, D.; Pekel, F.; Özkar, S. Improved adhesive properties and bonding performance of HTPB-based polyurethane elastomer by using aziridine-type bond promoter. *J. Appl. Polym. Sci.* **2001**, *80*, 806–814.
- (9) Sandén, R.; Wingborg, N. Bonding a HTPB liner to modern rocket case materials. *J. Appl. Polym. Sci.* **1989**, *37*, 167–171.
- (10) Grythe, K. F.; Hansen, F. K. Surface modification of EPDM rubber by plasma treatment. *Langmuir* **2006**, *22*, 6109–6124.
- (11) Zhou, Q.-C.; Xu, J.-S.; Chen, X.; Zhou, C.-S. Review of the adhesively bonded interface in a solid rocket motor. *J. Adhes.* **2016**, *92*, 402–428.
- (12) Zhang, G.; Li, J.; Sun, S.; Luo, Y. Azido-terminated Hyperbranched Multi-arm Copolymer as Energetic Macromolecular Plasticizer. *Propellants, Explos., Pyrotech.* **2019**, *44*, 345–354.
- (13) Teimuri-Mofrad, R.; Safa, K. D.; Abedinpour, S.; Rahimpour, K. Synthesis of 5-(Dimethylsilyl) pentylalkylferrocene-grafted HTPB (alkylFc-HTPB) via Platinum-catalyzed Hydrosilylation. *J. Iran. Chem. Soc.* **2017**, *14*, 2177–2185.
- (14) Xiao, F.; Feng, F.; Li, L.; Zhang, D. Investigation on ultraviolet absorption properties, migration, and catalytic performances of ferrocene-modified hyper-branched polyesters. *Propellants, Explos., Pyrotech.* **2013**, *38*, 358–365.
- (15) Ünver, A.; Dilsiz, N.; Volkan, M.; Akovali, G. Investigation of acetyl ferrocene migration from hydroxyl-terminated polybutadiene based elastomers by means of ultraviolet–visible and atomic absorption spectroscopic techniques. *J. Appl. Polym. Sci.* **2005**, *96*, 1654–1661.
- (16) Gottlieb, L. Analysis of DOA migration in HTPB/AP composite propellants. *Energ. Mater. Anal., Charact. test Tech.* **1994**, *90–91*.
- (17) Dilsiz, N.; Ünver, A. Characterization studies on aging properties of acetyl ferrocene containing HTPB-based elastomers. *J. Appl. Polym. Sci.* **2006**, *101*, 2538–2545.
- (18) Grythe, K. F.; Hansen, F. K. Diffusion rates and the role of diffusion in solid propellant rocket motor adhesion. *J. Appl. Polym. Sci.* **2007**, *103*, 1529–1538.
- (19) Grythe, K. F.; Hansen, F. K.; Olsen, Tr. Adhesion in solid propellant rocket motors. *J. Adhes.* **2007**, *83*, 223–254.
- (20) Zhang, B. W.; Li, X. Y.; Zhang, W. H.; Ren, R.; Zhang, Z. B.; Luo, Y. J. Preparation of anti-migration transition layer and its application in cast-in-case solid rocket motors. *J. Appl. Polym. Sci.* **2021**, *138*, No. 50680.
- (21) Zhang, Z.; Luo, N.; Wang, Z.; Luo, Y. Polyglycidyl nitrate (PGN)-based energetic thermoplastic polyurethane elastomers with bonding functions. *J. Appl. Polym. Sci.* **2015**, *13223* DOI: 10.1002/app.42026.
- (22) Agrawal, J.; Bouzon, J.; Vergnaud, J. Modelling of nitroglycerine and water migration behaviour through unsaturated chloropolyesters. *Polymer* **1989**, *30*, 1488–1492.
- (23) Agrawal, J.; Bouzon, J.; Vergnaud, J. Study of kinetics of nitroglycerine and water migration through semi-rigid unsaturated polyesters. *J. Polym. Eng.* **1990**, *9*, 53–66.
- (24) Piringer, O. G.; Baner, A. L. *Plastic Packaging Materials for Food: Barrier Function, Mass Transport, Quality Assurance, and Legislation*; John Wiley & Sons, 2008.
- (25) Weibull, W. A Statistical Theory of the Strength of Materials IVA. *Ingenioersvetenskapskad. Handl.* **1939**, *151*, 0.
- (26) Weibull, W. A Statistical Distribution Function of Wide Applicability. *J. Appl. Mech.-Trans. ASME* **1951**, *18*, 293–297.
- (27) Poças, M. d. F.; Oliveira, J. C.; Pereira, J. R.; Brandsch, R.; Hogg, T. Modelling migration from paper into a food simulant. *Food Control* **2011**, *22*, 303–312.
- (28) Helmroth, E.; Rijk, R.; Dekker, M.; Jongen, W. Predictive modelling of migration from packaging materials into food products for regulatory purposes. *Trends Food Sci. Technol.* **2002**, *13*, 102–109.
- (29) Limm, W.; Hollifield, H. C. Modelling of additive diffusion in polyolefins. *Food Addit. Contam.* **1996**, *13*, 949–967.
- (30) Poças, M. F.; Oliveira, J. C.; Brandsch, R.; Hogg, T. Analysis of mathematical models to describe the migration of additives from packaging plastics to foods. *J. Food Process Eng.* **2012**, *35*, 657–676.
- (31) Brecht, J.; Chau, K.; Fonseca, S.; Oliveira, F.; Silva, F.; Nunes, M.; Bender, R. Maintaining optimal atmosphere conditions for fruits and vegetables throughout the postharvest handling chain. *Postharvest Biol. Technol.* **2003**, *27*, 87–101.
- (32) Sánchez-Adsuar, M. Influence of the composition on the crystallinity and adhesion properties of thermoplastic polyurethane elastomers. *Int. J. Adhes. Adhes.* **2000**, *20*, 291–298.
- (33) Byrd, J.; Guy, C. Destructive Effects of Diffusing Species in Propellant Bond Systems, 21st Joint Propulsion Conference, 1985; p. 1438.
- (34) Crank, J. *The Mathematics of Diffusion*; Oxford University Press, 1979.
- (35) O'connell, P.; McKenna, G. Large deformation response of polycarbonate: Time-temperature, time-aging time, and time-strain superposition. *Polym. Eng. Sci.* **1997**, *37*, 1485–1495.
- (36) Tingfang, S.; Bohua, Z. Master Curve for the Prediction of Service Life of Solid Rocket Grain. *Acta Armamentarii* **1998**, *4*.
- (37) Deng, B.; Xie, Y.; Tang, G. J. Three-dimensional Structural Analysis Approach for Aging Composite Solid Propellant Grains. *Propellants, Explos., Pyrotech.* **2014**, *39*, 117–124.
- (38) Duncan, E. Characterization of a glycidyl azide polymer composite propellant: Strain rate effects and relaxation response. *J. Appl. Polym. Sci.* **1995**, *56*, 365–375.
- (39) Wang, Z. J.; Qiang, H. F.; Wang, G. Experimental Investigation on High Strain Rate Tensile Behaviors of HTPB Propellant at Low Temperatures. *Propellants, Explos., Pyrotech.* **2015**, *40*, 814–820.
- (40) Wang, Z.; Qiang, H.; Wang, G. Experimental investigation on high strain rate tensile behaviors of HTPB propellant at low temperatures. *Propellants, Explos., Pyrotech.* **2015**, *40*, 814–820.